Supplementary Information for:

Polar-nonpolar interconnected elastic networks with increased permittivity and high breakdown fields for dielectric elastomer transducers

Carmen Racles*[1], Adrian Bele[1], Mihaela Dascalu[1], Valentina Musteata[1], Cristian Dragos Varganici[1], Daniela Ionita[1], Stelian Vlad[1], Maria Cazacu[1], Simon J. Dünki [2], Dorina M. Opris*[2]

[1]*Petru Poni Institute of Macromolecular Chemistry, Aleea Grigore Ghica Voda 41A, Iasi, 700487, Romania.*

[2]*Empa, Swiss Federal Laboratories for Materials Science and Technology, Laboratory for Functional Polymers, Ueberlandstr. 129, CH-8600, Dübendorf, Switzerland.*

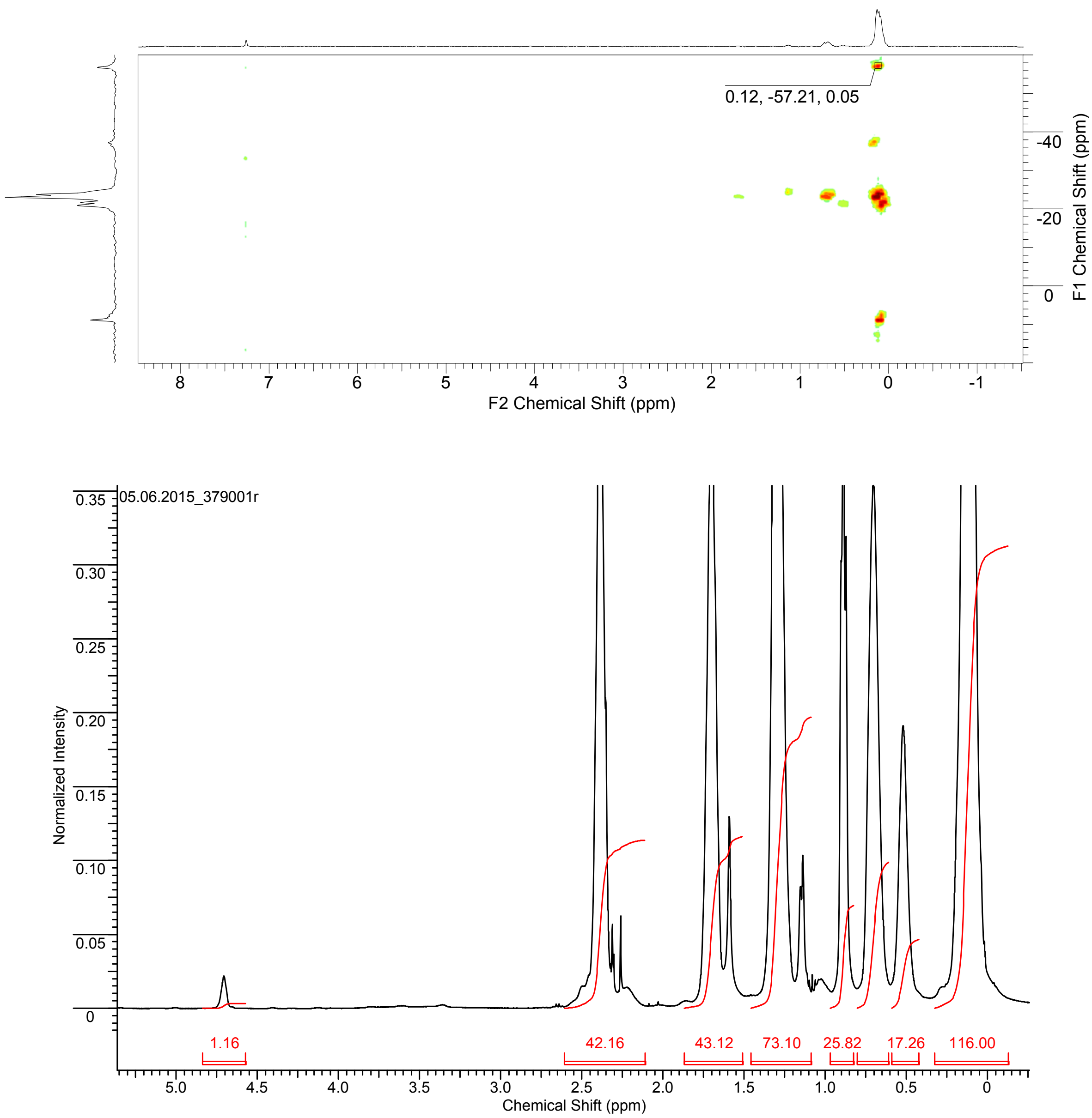

Figure S1: ^{29}Si NMR and ^{1}H NMR spectra of a partially cross-linked copolymer (P_{62}). The signal at -57 ppm in the ^{29}Si spectrum is assigned to trifunctional siloxane, while the Si-H signal is seriously diminished (for comparison see Figure S5b).

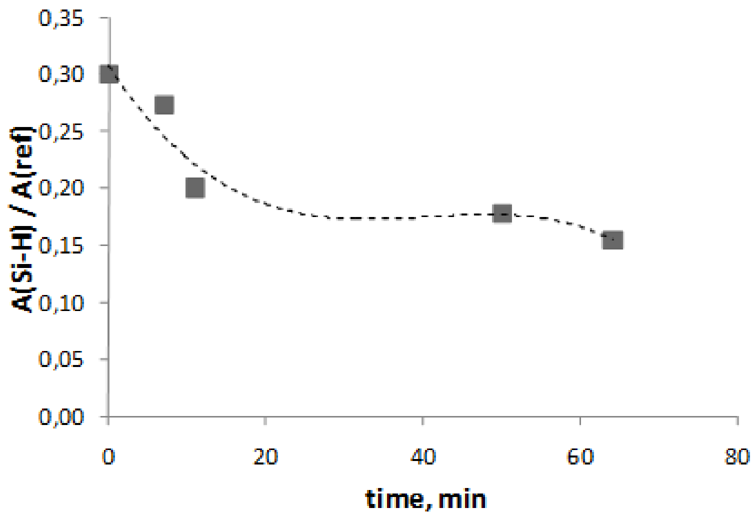

Figure S2: Reaction monitoring with IR spectroscopy: variation of the Si-H stretching band at 2154 cm^{-1} versus $Si\text{-}CH_3$ symmetric band at 1260 cm^{-1} due to hydrolysis of $\mathbf{P_{62}}$ as function of time.

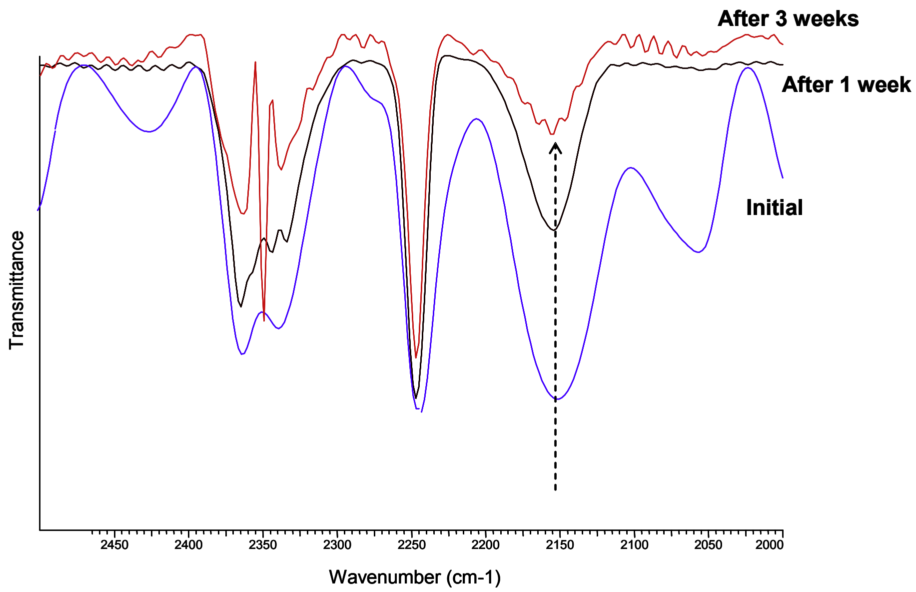

Figure S3: Evolution of the Si-H stretching band in a cross-linked film within three weeks.

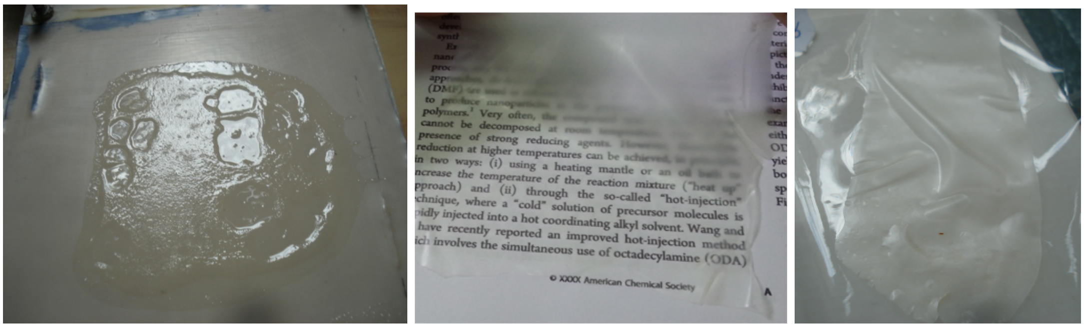

Figure S4: Image of a blend of cross-linked PDMS and P_{62} (left), $\mathbf{P_{62}(1/3)}$ (middle) and $\mathbf{P_{62}^{part}(1/2)}$ (right). , Macroscopic phase separation can be seen when P_{62} is not cross-linked (the left-side photo).

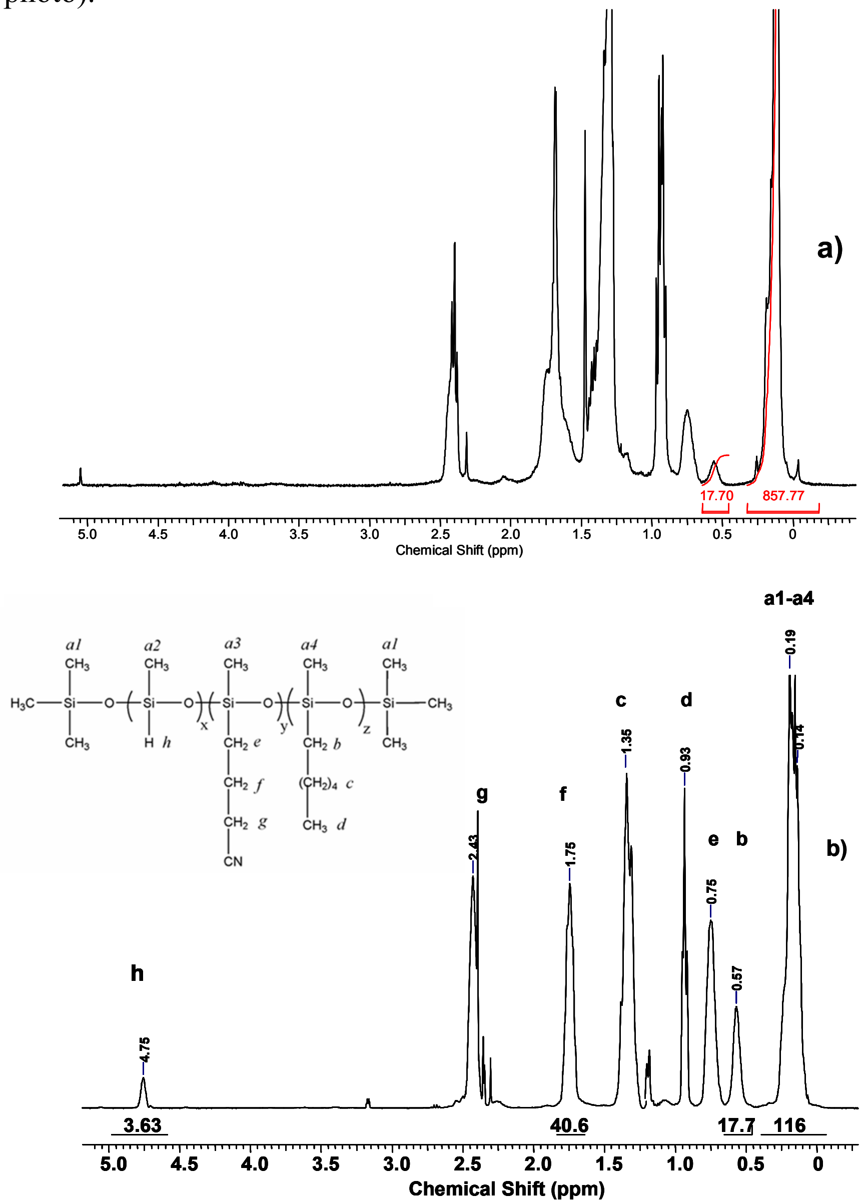

Figure S5: ^{1}H NMR spectrum of the extract from film $P_{62}(1/2)$ (a), compared with the starting copolymer (b). The ratio between the Si-CH_2 and Si-CH_3 protons indicate that the extract contains little amount of un-cross-linked P_{62} and a high amount of un-cross-linked PDMS (possible macrocycles) –roughly 1:7.4. A large amount of DBDTL catalyst is, as expected, present in the extract. No signal for Si-H protons can be seen.

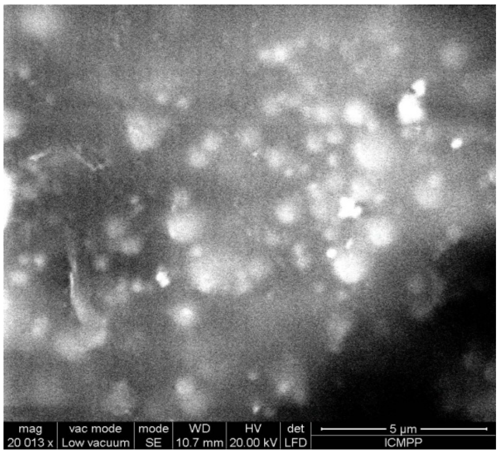

Figure S6: SEM image of cross-section of material $\mathbf{P_{62}^{part}(1/2)}$.

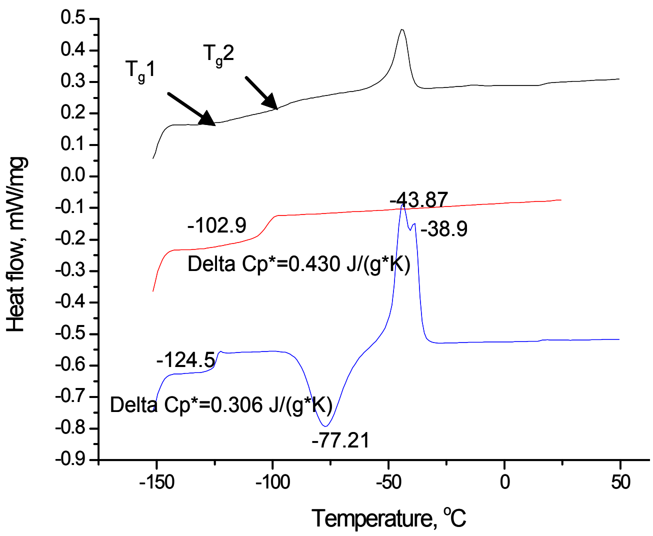

Figure S7: DSC scans (second heating) of $\mathbf{P_{10}}$ (red), PDMS (blue) and $\mathbf{P_{10}(1/2)}$ (black).

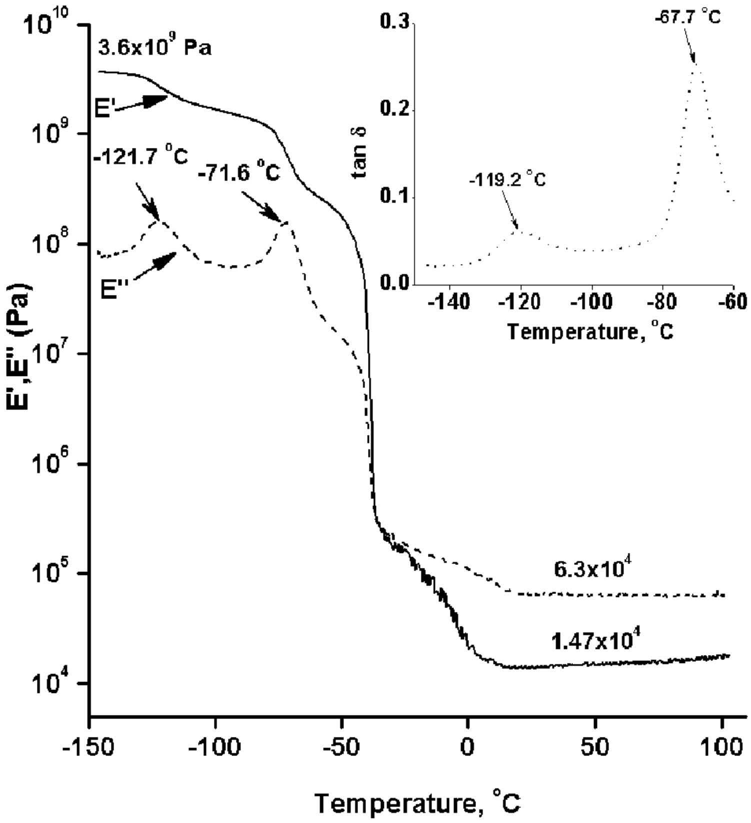

Figure S8: DMA curves of **P_{62}(1/2)** in tension mode, at 1 Hz, at a heating rate of 2 °C/min.

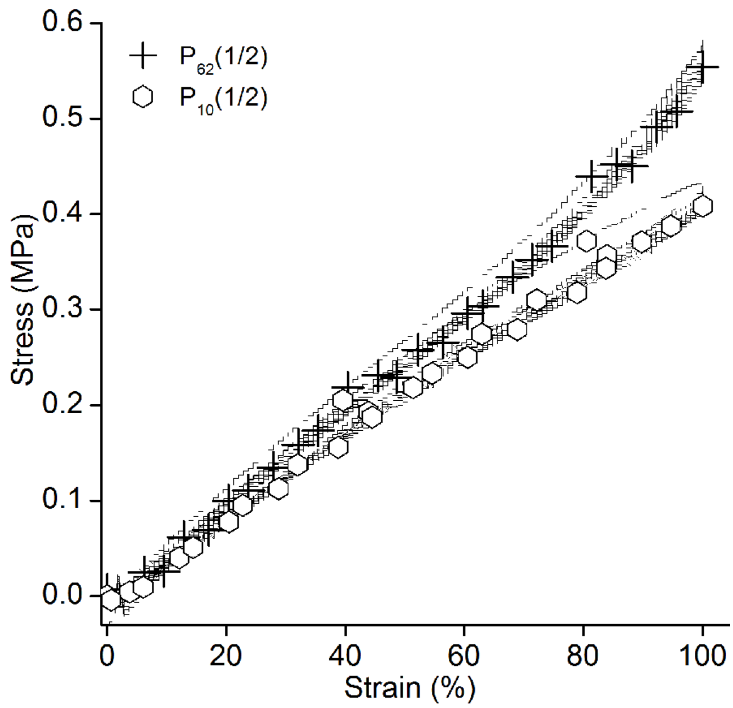

Figure S9: The cyclic test results for materials **P_{62}(1/2)** and **P_{10}(1/2)**.

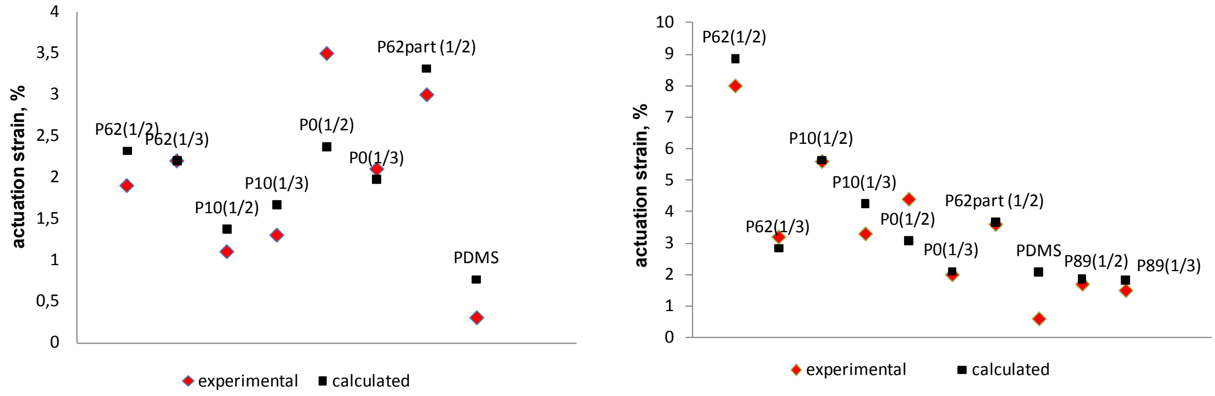

Figure S10: Calculated and experimental actuation strain at 30 V/µm (left) and at breakdown (right)

Table S1: Mechanical properties of the optimized materials compared to the corresponding ones with similar composition.

Sample	Young modulus (MPa)				Tensile strength [MPa]	Elongation at break [%]
	10%	20%	50%	100%		
P_{62}(1/3)	0.75	0.62	0.41	0.39	1.02	208
$^{soft}P_{62}$(1/3)	0.28	0.21	0.67	0.50	1.19	350
P_{62}^{part}(1/2)	0.48	0.45	0.46	0.70	1.71	247
$^{soft}P_{62}^{part}$(1/2)	0.14	0.32	0.20	0.48	0.63	489

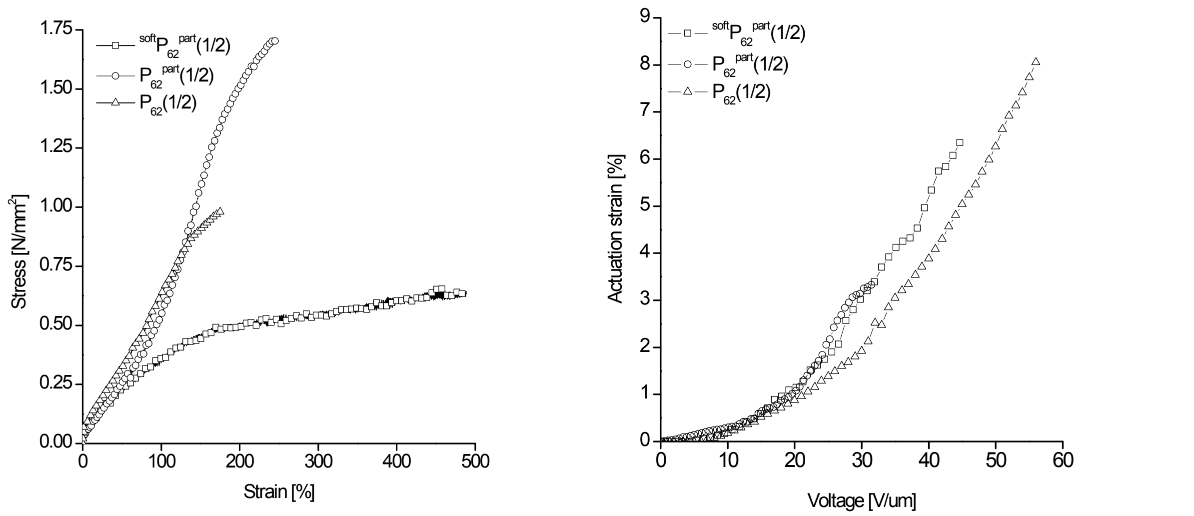

Figure S11: Stress-strain curve (left) and electromechanical response (right) of all-polymer composites compared with the interconnected network with similar composition.